Large Satellite Constellations and Their Potential Impact on VGOS Operations

Federico Di Vruno[1], Vincenza Tornatore[2]

Abstract Large LEO satellite constellations (or so-called Megaconstellations) will significantly change the view of the sky in some radio frequency bands. For VGOS telescopes, it is important to understand the potential impact these constellations will have on their operations, what the risk is of its receivers going into non-linear behavior, and how much additional power a telescope would receive if observing in the same frequencies where satellites are transmitting. This work describes three of these new constellations (as they would look fully deployed) and summarizes the results of a particular study considering two VGOS telescopes (Onsala and Wettzell).

Keywords VGOS, RFI, Megaconstellations, satellite constellations

1 Introduction

The industrialization of spacecraft construction and the lowering in costs of space launches have paved the way for big plans in Low Earth Orbit (LEO). Large satellite constellations like Starlink phase 1 (with 4,400 satellites) and OneWeb phase 1 (with 648 satellites) are already in the deployment phase. Others like Project Kuiper (from Amazon) or Guowang (from China) are in their development phase and yet others with even larger numbers are being filed into the International Telecommunication Union (ITU) system (see Table 1). With altitudes between 500 km and 1,200 km, these new constellations will surround the planet almost homogeneously. From a radio telescope point of view, the situation in the sky will change considerably. This change is already evident in the number of active satellites in LEO, from about 2,000 in 2018, to more than 5,000 in 2022, and the trend suggests that it may reach hundred of thousands in this decade [5].

Until now, most of the satellites for internet communication were located in the geostationary belt (at approximately 35,780 km altitude), appearing fixed in the sky for a terrestrial observer [7]. The new LEO satellites will orbit the Earth with a period of about 90 minutes and will be seen as hundreds to thousands of bright and fast-moving radio sources in the sky with downlinks in frequency bands from 10.7 GHz up to 76 GHz (see Section 2.2).

Contrary to the situation with terrestrial radio frequency interference (RFI), it is not possible to build radio telescopes far away from satellite transmissions [1]. The challenge is further increased by the opposite pointing direction of the radio telescopes and the user downlink antenna beams.

The typical power flux density (PFD) of satellite constellations is in the order of -146 dBW/m^2 [12, 6] in 4 kHz or an equivalent to 62×10^6 Jy, i.e., more than seven orders of magnitude brighter than a typical VGOS source [8]. These strong signals will require a radio astronomy receiver to have a large dynamic range to accommodate the RFI and still be able to detect faint cosmic sources in other frequency channels within the receiver band. This is normally possible for modern radio astronomy receivers. But it can be different in some particular situations such as total power bolometric receivers or receivers with a low effective number of bits (ENB) [3].

1. SKA Observatory, Jodrell Bank, Manchester, United Kingdom
2. Politecnico di Milano, DICA, Milano, Italy

2 Large LEO Constellations

Radio astronomy has been dealing with satellite transmissions since the very first satellites were launched back in the 1960s. Implementing different strategies, such as using analog receivers with large dynamic ranges, smart scheduling, and RFI flagging among others, radio telescopes have been more or less able to mitigate (or avoid) the effect of these strong radio transmissions towards Earth [1]. In conjunction with these strategies, spectrum management has also played a key role in dealing with the effects of satellites. Several radio astronomy groups have worked at regional, national, and international levels for the protection of the radio astronomy service (RAS) frequency bands allocated by the ITU. Some had successful results like the GLONASS example, while others are in battles that are ongoing for 20 years since satellite deployment like in the IRIDIUM case [2].

Table 1 Some of the large LEO constellations in deployment or planned.

Constellation	Number of Satellites	Altitude [km]
Starlink Phase 1	4,400	550
OneWeb Phase 1	648	1,200
Amazon Phase 1	3,200	~ 600
Guowang (GW)	13,000	590 to 1,145
Starlink VLEO	7,600	340
Telesat	298	1,000
Starlink Phase 2	30,000	328 to 614
OneWeb Phase 2	6,372	1,200
Cinnamon–937	327,320	550 to 643

The exponential growth in the number of active satellites in Low Earth Orbit [5] could result in more than 2,000 satellites above the local horizon at any moment in time. Radio telescopes are sensitive to any transmitter in line of sight through its main beam or antenna sidelobes.

2.1 Walker-Delta Constellations

All these new constellations follow a "Walker Delta" type of distribution, composed of orbital *shells* at a certain altitude. Each shell contains several *orbital planes*, with a certain inclination with respect to the equator and distributed homogeneously over the 360 degrees of right ascension. Each one of the constellation's planes contains N satellites. A representation of Starlink Phase 2 is given in Figure 1.

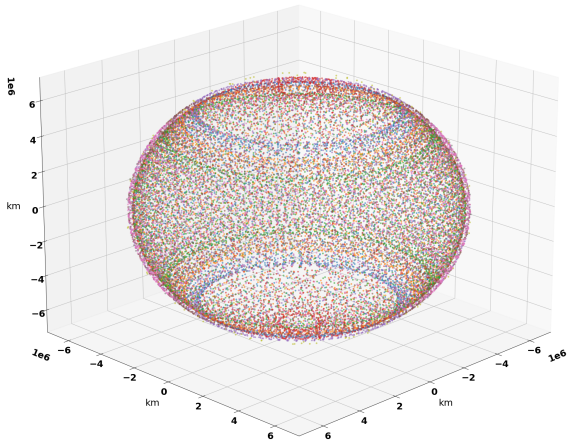

Fig. 1 View of Starlink Phase 2 constellation with 30,000 satellites. Different colors are used for each of the shells of the constellation frequency bands used by some of the satellite constellations.

A shell of a Walker-Delta constellation [17] is described by $i = t/p/f$ where i is the inclination, t is the total number of satellites, p is the number of equally spaced planes, and f is the relative spacing between satellites in adjacent planes. This description makes it very simple to simulate any of these constellations with the purpose of studying its geometric distribution in LEO as well as its effect on radio telescopes. It is also possible to use existing Two-Line Elements (TLEs) to obtain the approximate position of existing satellites in space, which can be useful to compare observations to simulation.

Figure 2 shows a qualitative view of the sky from the Wettzell VGOS station (lat 49 degrees), with the position of different satellite constellations simulated for 100 seconds. It is easy to see how the density of satellites in the sky will drastically change in the near future if all planned constellations are deployed.

2.2 Radio Frequencies

Satellite constellations transmit their downlink signals in frequencies allocated to the Fixed Satellite Service

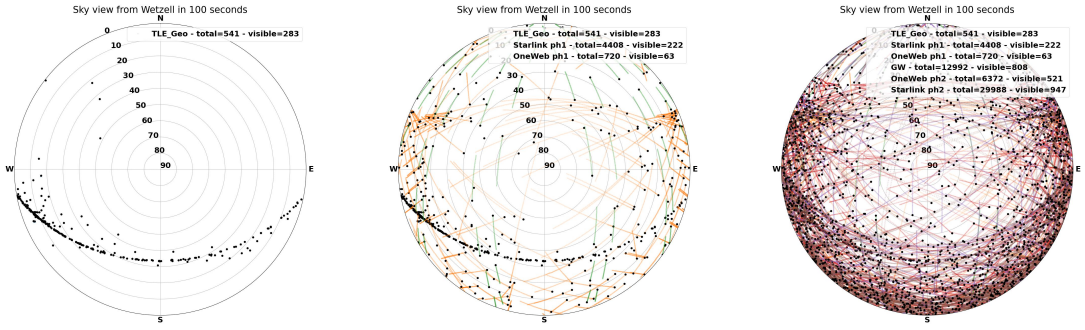

Fig. 2 Sky view from the Wettzell VGOS station with only geostationary satellites (left), simulation of SL1 and OW1 constellations fully deployed (middle), and simulation of six large LEO constellations fully deployed (right). The term "visible" is used for satellites above the horizon, as radio telescopes can detect satellites in any direction in the sky.

(FSS). Table 2 contains some of the currently in-use and planned FSS bands. It is important to note the proximity to some ITU protected RAS bands immediately adjacent or in very close proximity.

Table 2 Frequency bands used by some of the satellite constellations.

Frequency	Band name	Protected RAS bands (primary)
10.7–12.75 GHz	Ku	10.6–10.7 GHz
19.7–20.2 GHz	Ka	22.21–22.5 GHz
37.5–42.5 GHz	V	42.5–43.5 GHz
71.0–76.0 GHz	E	76–77.5 GHz

The close vicinity of the satellite's downlinks to radio astronomy bands is a matter of concern for radio astronomers and spectrum managers. For example, the protection of the 10.6–10.7 GHz Radio Astronomy Service (RAS) band, which includes a *passive band* in 10.68–10.7 GHz protected by the footnote RR No. 5.340 in the ITU-R Radio Regulations (RR), was studied for the Starlink Ph1 and OneWeb Ph1 constellations in [4]. The conclusion of the study was that both systems should not use the first 250-MHz channel to protect the RAS band. These signals cannot only impact sensitive observations in the RAS protected bands, but they can also affect wideband receivers which include the frequency range of user downlinks. Such wideband receivers (from 2 to 14 GHz in the case of VGOS) are necessary to conduct cutting-edge science or geodesy [8].

This paper focuses on the downlink frequency range 10.7 to 12.75 GHz where both OneWeb and Starlink have divided the band into eight channels of 250 MHz each. The study can be replicated for higher frequency bands with the appropriate modification of satellite and telescope characteristics.

3 Potential Impact on VGOS

By using large reflector antennas pointed towards the sky and wideband receivers covering the frequency range 2 to 14 GHz [8], VGOS telescopes can be impacted by downlinks of the large satellite constellations in different ways. In fact, the VGOS bandwidth is wide, while the protected radio astronomy band is very narrow, and Starlink and OneWeb use a considerable portion of the frequency spectrum. The severity of this impact depends on the interaction between the radio telescope beam and the satellite downlink beams. One of the most important aspects is how much a correlated baseline can be affected as the primary product of a VGOS observation. Nevertheless, the multidimensionality of this problem requires an analysis of the complete signal reception mechanisms and how each part of the signal chain may be impacted.

In a typical VGOS schedule, targets are observed with durations in the order of seconds to tens of seconds. The position of the target in the local sky and the density of satellites deployed will define how much interference will be seen by the telescope. The instantaneous received power from all satellites above the horizon may saturate the analog signal chain (e.g., low noise amplifiers, mixers), causing non-linearities

that would render the complete receiver band unusable, even if the digitizer band is tuned to a completely different frequency than the satellite downlinks channels. If the RFI power is not as strong and the analog signal chain remains linear, then there can be two possible scenarios:

- First scenario: the observed band is outside of the satellite downlink frequency range. In this case out-of-band emissions from the satellites could be a problem depending on their level. This work is not focusing on this, but [4] has studied that case.
- Second scenario: the observing band falls within one satellite downlink band (250 MHz channels) or vice versa. Strong RFI will be received by the VGOS antenna. This RFI can potentially be mitigated by correlation as long as the number of bits in the digitizer are enough to correctly digitize the signal. Since a VGOS digitizer has only two bits, the total integrated RFI needs to be lower (practically at least 10 dB lower or $1/10$) than the integrated noise power of the receiver [3].

Non-linearities and lack of headroom for RFI are transient phenomena and can be considered in terms of a data loss associated with the moments when a satellite is going through the main beam of the radio telescope. The issue of out-of-band emission is related to long integrations and needs a comparison between the level of integrated RFI vs. the integrated level of the astronomical source under observation. The following section describes a simulation method and presents a particular case for the Starlink phase 1, OneWeb phase 1, and Starlink phase 2 constellations to estimate data loss due to strong received power and the total aggregated RFI. The effects of the correlation are not included in this work but are currently under study by the authors.

4 Simulation Methodology

The simulation is based on the Equivalent Power Flux Density (EPFD) concept (see [11]), where the satellite constellation is propagated for a defined time duration, obtaining the coordinates and attitude of every satellite for each time step. Then the telescope antenna is pointed towards a defined *sky-cell* in azimuth and elevation, and for each of the simulated time steps the received power from all satellites above the horizon is calculated with the formula:

$$P_{rx_{(t,p)}} = \sum_{i=0}^{N_{sat}} (PFD_{sat_{(i,t)}} * A_{eff_{RAS_{(i,t,p)}}}) \qquad (1)$$

where:
t = time step
p = pointing direction
i = satellite index
PFD_{sat} = Satellite power flux density in W/m^2 towards the telescope location
$A_{eff_{RAS}}$ = Effective area of the telescope antenna in m^2 towards the satellite position

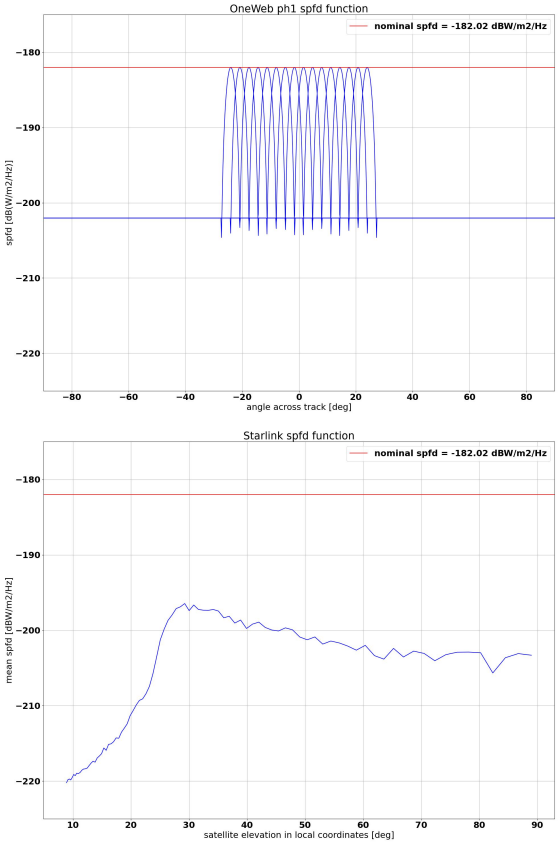

Fig. 3 OneWeb SPFD model (top) and Starlink SPFD model (bottom). The red line marks the maximum SPFD level of -182 dB/m^2/Hz.

This calculation is iterated for a number of *trials* (typically hundreds to thousands), where each try has a random start time of the constellation and, therefore, contributes to a statistically representative result. In sit-

uations where multiple frequencies are calculated, for example in the case of OneWeb with its 16 fixed-beams antenna (see Figure 3), the number of channels is added to the result. Therefore, the final calculation results in a data cube with four dimensions, namely the number of iterations N_{iters}, the number of pointing directions $N_{pointing}$, the number of time steps N_{time}, and the number of channels $N_{channel}$.

Although the original EPFD calculation as defined by the ITU uses telescope pointings in local coordinates (Alt, Az), this work considers pointings in celestial coordinates (Ra, Dec), because this allows to understand how celestial positions in different declinations can be impacted by satellite constellations transmissions.

4.1 Satellite Position Propagation

Using the Python package Cysgp4 [18] and the Astropy Coordinates package [14], the position of the satellites in horizontal coordinates (Alt, Az) and sky coordinates (Ra, Dec) are calculated for each timestep and each iteration (see Figure 5).

4.2 Satellite Power Flux Density (PFD)

The PFD from each satellite in a constellation is modeled based on publicly available information (ITU documents and FCC filings). To calculate the power flux density towards the telescope site, the coordinates of the telescope in the satellite reference frame are also calculated using the Python package cysgp4 [18].

OneWeb satellites are modeled based on the information available in the ECC report 271 [4], with eight channels in the range 10.7–12.75 GHz. A fixed beam antenna pattern, like the OneWeb system, makes it simpler to calculate the received power in a deterministic way.

The PFD from Starlink satellites is more complex to model since they have an antenna array that can produce, and electronically steer, several beams in one or multiple frequency channels. The mean PFD from a Starlink satellite is modeled as a function of the elevation of the satellite, obtained from a Monte-Carlo simulation in which the steering angle, the number of beams, and the position of satellite and observer were varied a large number of times. Starlink satellites are modeled as one frequency channel at a time.

4.3 Radio Telescope Antenna

The radio telescope antenna is modeled based on [10]. While this model is not a real measurement of the antenna pattern of a radio telescope, it is based on real measurements and is considered as a worst case for compatibility studies. To obtain the gain towards the satellite, the angle between the pointing direction and the position of the satellite is calculated.

The effective area of the antenna is calculated with the following equation:

$$A_{eff} = G_{RAS} * (\lambda^2/(4*\pi)) \quad (2)$$

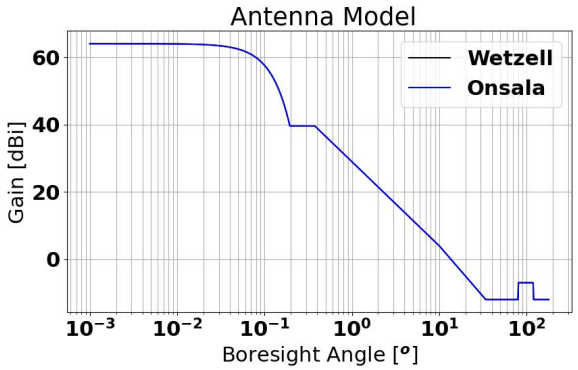

Fig. 4 Antenna pattern as defined in ITU-R RA.1631.

4.4 Correlation

Interferometry can greatly mitigate the effects of RFI, especially when the baselines are long like in the case of VLBI [16]. Although Thompson et al. have studied the effect that long baselines have over single (and stationary) RFI transmitters, the situation is not the same when potentially hundreds of transmitters using the same frequency and bandwidth are received simultaneously as can happen now.

For example in [7], Petrachenko identifies the 10.7–12.75 GHz range as a usable frequency range as only geostationary satellites were using that frequency at that time. Now the received RFI signal at an antenna will be the sum of the signals from all satellites above the horizon (of course, with different levels of attenuation). Such an analysis is deferred to a future update of this work.

4.5 Saturation Limit Threshold

Digital processing operations in a radio telescope can be applied as long as the analog and digital signal chains behave in a linear manner; strong enough signals will generate non-linearities corrupting the complete receiver band for the duration of the interference. Defining the level when a receiver goes non-linear is not a simple task and will depend on each particular receiver. In the case of the VGOS receivers a conservative value for total power of -50 dBm is considered to keep the analog signal chain within the linear regime.

If the received power is below this linearity threshold, the analog signal can then be correctly digitized with a bandwidth of 1 GHz. Two scenarios can be identified:

1. Digitizing a frequency range outside of 10.7–12.75 GHz. This should not have any complications since the signal chain behaves in a linear way. Therefore, this case will not be further studied.
2. Digitizing in a frequency range within 10.7–12.75 GHz. In this case it is interesting to understand when the RFI produces a significant amount of power compared to the RMS noise of the receiver.

Given the distinct characteristic of the VGOS system to use a 2-bit correlator, it is reasonable to consider that there is not much headroom in the digital signal chain to accommodate for RFI. This work considers that any signal above or equal to the receiver's noise power will result in a data loss. This defines the second threshold as a spectral power flux density equal to the RMS noise of a 20-K receiver system (-215 dBW/Hz).

These two thresholds are used in the simulation: a first set of flags is produced when the total integrated power (considering the eight channels of 250 MHz for each constellation) is higher than -50 dBm (representing a total data loss) and the second one representing a data loss in the case of observing in the same frequency range as the satellite transmissions.

After these two flagging stages, low level RFI will still be present. It is of interest to understand how this will affect the correlation of the baseline. This will be further studied in a future update of this work and compared to the thresholds defined in RA.769 [9].

4.6 Metrics

Based on the threshold limits defined in the previous section, the following metrics are used:

1. Full Band Data Loss (**FBDL**): percentage of time that the complete band is lost due to very strong RFI, where the total received power is > -50 dBm.
2. Digitizer Data Loss (**DDL**): percentage of the total observation time (single run multiplied by the number of iterations) that the instantaneous power spectral density is above 10% of the integrated noise power of the receiver. This can be calculated as a function of the declination of the source.
3. Average Equivalent Spectral Power Flux Density (**aESPFD**): average value of the equivalent Spectral Power Flux Density (eSPFD) during the observation time in each antenna. The eSPFD is calculated as the received spectral power flux density [W/m^2/Hz] divided by the maximum effective antenna area, and it is useful to compare to the SPFD (in units of Jy) of a celestial source in the main beam of the antenna.

5 Case Study Simulation

A specific study case was selected to understand the impact from several satellite constellations on two telescopes normally involved in VGOS observations. It is the intent to further expand this work into how correlation over the long baseline mitigates the RFI. The VGOS stations in Sweden (Onsala Space Observatory) and Germany (Geodetic Observatory Wettzell) were selected as the test stations using the parameters of Table 3 and the constellations Starlink phase 1, OneWeb phase 1, and Starlink phase 2 (Table 4). The simulated observations were run for 100 seconds in one-second timesteps with 100 iterations.

Table 3 VGOS station parameters used for the simulation.

Station	Wettzell	Onsala
Location (lon, lat) (deg)	(12.88, 49.14)	(11.92, 57.39)
Height (m)	600	20
Antenna Diameter (m)	13	13
Antenna Efficiency (%)	80	80
Receiver bandwidth (MHz)	1000	1000
System Temperature (K)	20	20
ITU-R RA.769 threshold (dBW/m^2/Hz)	−240	−240

Table 4 Parameters of satellite constellations used for the study [12, 13, 6].

Constellation	Altitude	Inclination	Number of planes	Satellites per plane
Starlink ph 1	550	53	72	22
	540	53.2	72	22
	570	70	36	20
	560	97.6	6	58
	560	97.6	4	43
OneWeb ph 1	1200	87.9	18	40
Starlink ph 2	340	53	48	110
	345	46	48	110
	350	38	48	110
	360	96.9	30	120
	525	53	28	120
	530	43	28	120
	535	33	28	120
	604	148	12	12
	614	115.7	18	18

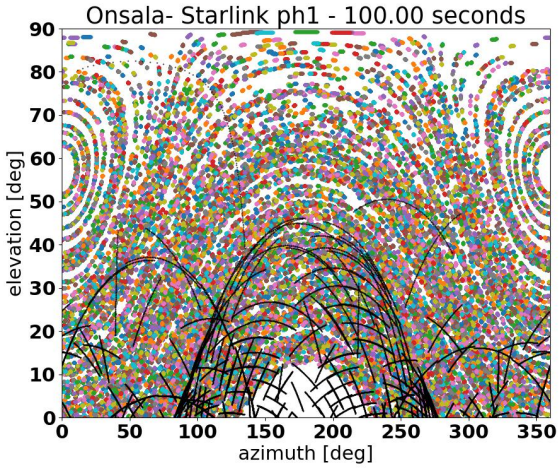

Fig. 5 Horizontal (Alt, Az) view of the pointing directions (in colors) and movement of the Starlink Phase 1 satellites (black) as seen from the Onsala Space Observatory for a time duration of 100 seconds.

Originally, we intended to use a real VGOS schedule, using the (Ra, Dec) values of the observed sources, but to get a more representative result of the impact as a function of source declination, the number of sources was increased artificially to 277 in a random fashion (see Figure 6 for a plot of the source distribution). Figure 5 shows the view of the local sky in (Alt, Az) and how the celestial sources and the satellite constellation (in this case Starlink Phase1) move across the sky in that timeframe.

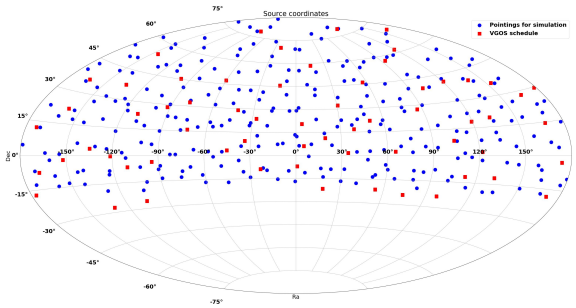

Fig. 6 VGOS schedule (2022Jan27) sources in red squares, selected telescopes pointings for the simulation in blue circles.

6 Results

The results for each one of the selected metrics are summarized here for each constellation simulated.

6.1 Full Band Data Loss (FBDL)

Notably, the analog saturation threshold was not reached due to the combination of maximum PFD from the satellites (−98 dBW/m^2 in 250 MHz) and maximum effective area of the VGOS antennas (106 m^2 or 20.3 dBm^2), as can be seen in Figure 7. This shows that even with large constellations such as Starlink phase 2 the analog receivers would still behave in a linear fashion.

6.2 Digital Data Loss (DDL)

When considering an observation coinciding in frequency with the downlinks of satellites (i.e., in within

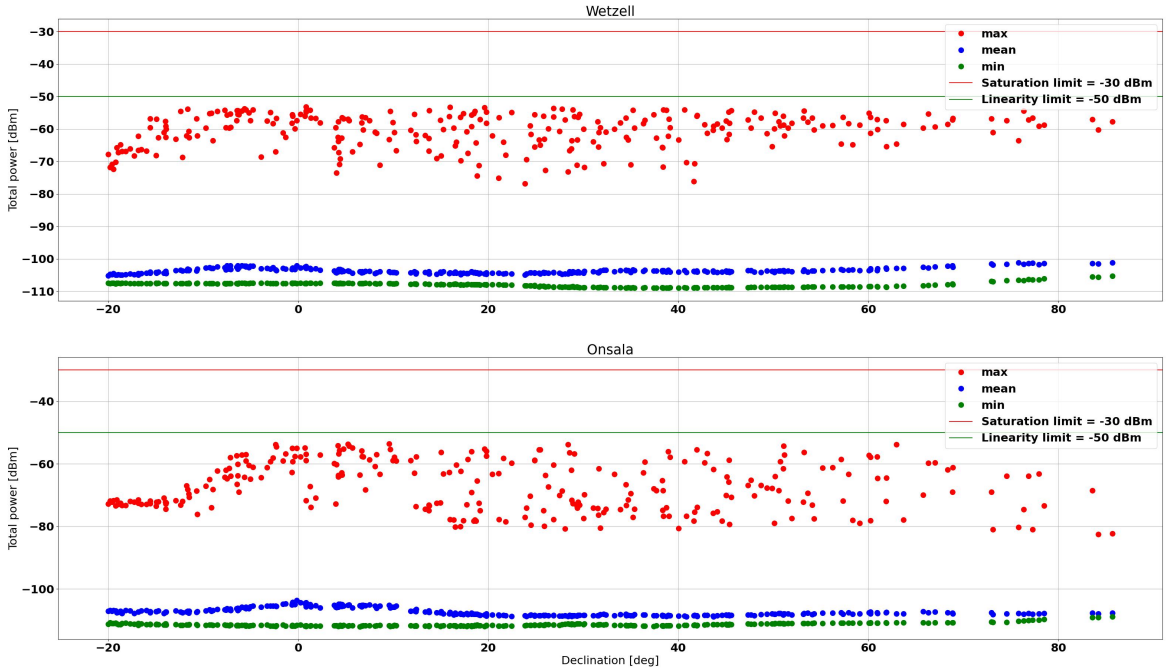

Fig. 7 Instantaneous power received by both VGOS antennas as a function of pointing declination with Starlink phase 2 constellation. The linearity threshold of −50 dBm was not reached in any situation.

the 10.7–12.75 GHz) the DDL varies as a function of declination of the observed source and observatory latitude. This effect is attributable to the different structures of each constellation's density of satellites around the Earth and the latitude of the observer. This shows that the impact on VGOS stations (and radio telescopes in general) strongly depends on the observatory latitude (Figure 8).

6.3 Average Equivalent Spectral Power Flux Density (aESPFD)

After a certain percentage of the observed data was lost as DDL (see Section 6.2), the aESPFD is calculated for each constellation as a function of declination. In this case the flagged percentage is calculated as the product of the flags from the previous section for each antenna.

Considering that the ITU-R RA.769 thresholds for harmful interference for VLBI are defined as -193 dBW/m^2/Hz, representing an ESPFD of 250 Jy for an antenna of 13 m in diameter, the results show that VGOS observations could in principle be conducted inside the satellite downlink bands considering the percentage of data lost (Figure 9).

7 Conclusions

This paper proposed metrics to evaluate the impact of large satellite constellations on VGOS operations by a simil-epfd simulation for Starlink ph1 and ph2, OneWeb ph1, and two European VGOS sites as receiving stations.

Through calculations and simulations it was proved that the maximum received power even in beam-to-beam coupling condition with satellites will not be enough to saturate the analog chain of a VGOS receiver. As for the digitized part, the simulations show that observations in the same band as the downlinks from satellites can have a significant percentage of data loss due to strong signals compared to the thermal noise of the receiver. Nevertheless, the results show that the ESPFD for both antennas and all constellations is lower than the threshold defined by ITU-R for VLBI. Observations outside of the satellite downlink

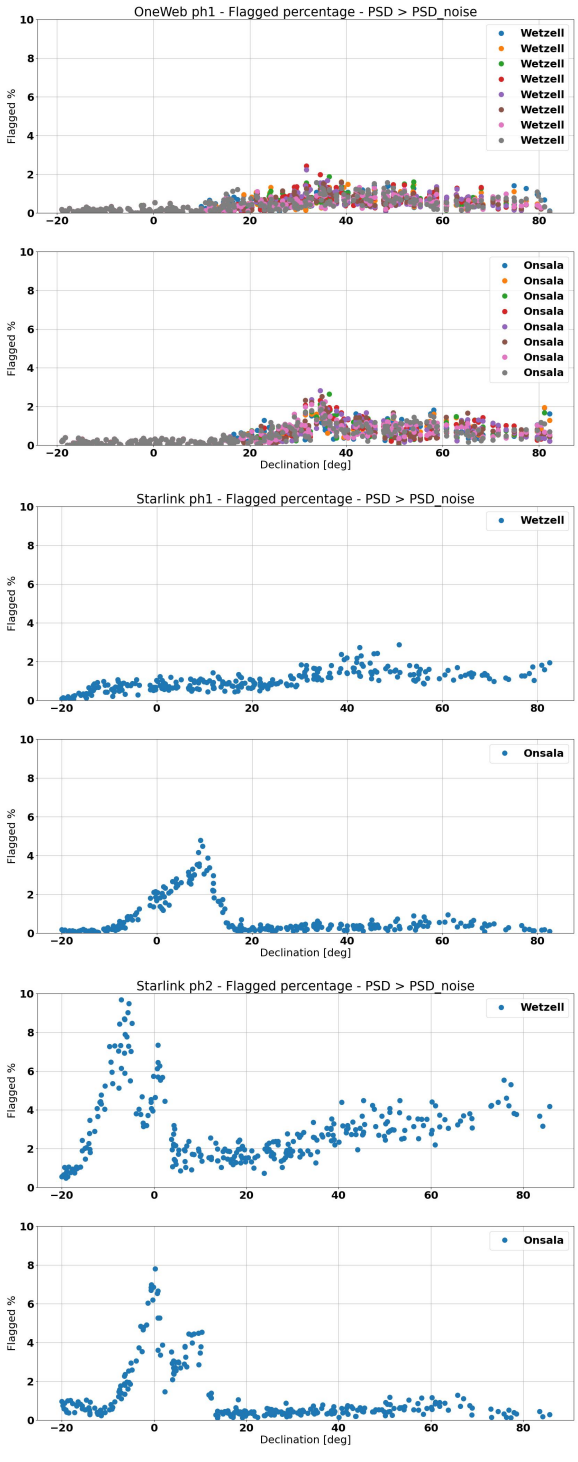

Fig. 8 Flagged percentage for each antenna and each constellation. A flag is raised when the power spectral density received is above the noise spectral density.

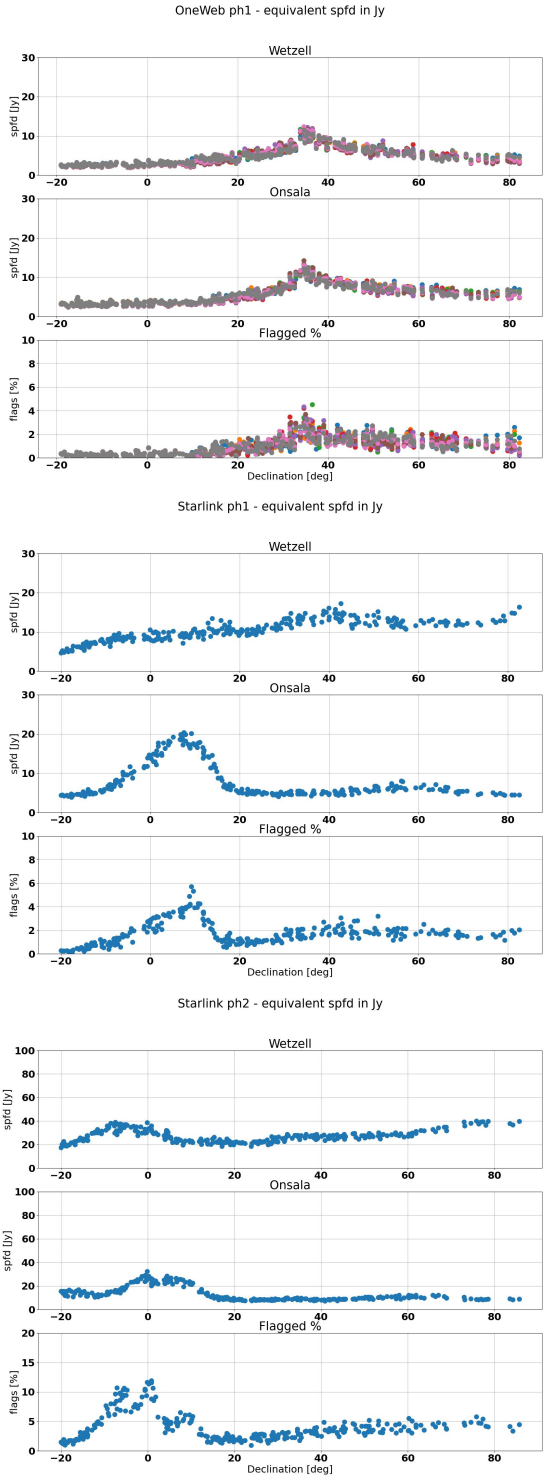

Fig. 9 Average Equivalent Spectral Power Flux Density (aESPFD) as a function of declination for each constellation.

bands should not be impacted by satellite downlinks in this frequency range.

As further work the authors will continue investigating how correlation can help mitigate the signals from satellite constellations and how the aggregation of all constellations scales the impact.

Acknowledgements

The authors would like to thank the IVS Coordinating Center at NASA Goddard Space Flight Center (GSFC) for taking the archive of IVS sessions. The schedule used in this work is available at the https://ivscc.gsfc.nasa.gov/sessions/2022/vo2027 web page. We are grateful to Salvo Buttaccio for the assistance with the VGOS schedule, to Dr. Benjamin Winkel for assistance with the use of the Cysgp4 Python package, and to Dr. Jose Antonio Lopez-Perez and Dr. Hayo Hase for useful discussions about VGOS receivers and operations.

References

1. W. A. Baan, 2011. “RFI mitigation in radio astronomy” RFI Mitigation Workshop 2010
2. J. Cohen, Iridium and Radio Astronomy in Europe Spectrum Management for Radio Astronomy: proceedings of the IUCAF summer school held at Green Bank, West Virginia, June 9–14, 2002.
3. Cooper, B.F.C., 1970. “Correlators with two-bit quantization”. Australian Journal of Physics, 23, pp. 521–527.
4. ECC Report 271, “Compatibility and sharing studies related to NGSO satellite systems operating in the FSS bands 10.7–12.75 GHz (space-to-Earth) and 14–14.5 GHz (Earth-to-space)”, European Communications Office, 2021.
5. A. Lawrence et al., 2022. “The case for space environmentalism”, Nature Astronomy, Vol. 6, pp. 428–435.
6. OneWeb phase 1 FCC filing, https://fcc.report/IBFS/SAT-MPL-20200526-00062/2379565
7. B. Petrachenko, “The Impact of Radio Frequency Interference (RFI) on VLBI2010”, IVS 2010 General Meeting Proceedings, pp. 434–438.
8. B. Petrachenko et al. 2010. “Final Report of the Observing Strategies Sub group of the IVS Working Group 3”, https://ivscc.gsfc.nasa.gov/about/wg/wg3/1_observing_strategies.pdf
9. Recommendation ITU-R RA.769 “Protection criteria used for radio astronomical measurements”
10. Recommendation ITU-R RA.1631 “Reference radio astronomy antenna pattern to be used for compatibility analyses between non-GSO systems and radio astronomy service stations based on the epfd concept”
11. Recommendation ITU-R S.1586 “Calculation of unwanted emission levels produced by a non-geostationary fixed-satellite service system at radio astronomy sites”
12. Starlink phase 1 FCC filing, https://fcc.report/IBFS/SAT-MOD-20200417-00037/2274316
13. Starlink phase 2 FCC filing, https://fcc.report/IBFS/SAT-AMD-20210818-00105
14. The Astropy Collaboration et al., “Astropy: A community Python package for astronomy”, A&A Volume 558, October 2013.
15. The Astropy Collaboration et al.,“The Astropy Project: Building an inclusive, open-science project and status of the v2.0 core package”, https://arxiv.org/abs/1801.02634
16. Thompson, 1982. “The Response of a Radio-Astronomy Synthesis Array to Interfering Signals”, IEEE Transactions on Antennas and Propagation, Vol. AP-30, No. 3, May 1982.
17. J. G. Walker, Satellite constellations, Journal of the British Interplanetary Society, Vol. 37, pp. 559–571, 1984.
18. B. Winkel, “A wrapper around the SGP4 package, for sat TLE calculations”, https://github.com/bwinkel/cysgp4